

# Detection of Relativistic Particles

Luke C. L. Yuan

Detection of high-energy particles at energies in the relativistic region is comparatively easy, and can be accomplished by a large number of methods. On the other hand, identification of these particles, and especially the ability to seek out a specific particle, is considerably more difficult, and only a few detectors can achieve it.

In the study of high-energy interactions, particles of various types are usually produced in the interaction process. To perform an experiment involving a particular type of particle, one must be able to select this particle and exclude all other particles which may be present. Such identification and selection of high-energy particles becomes increasingly difficult as the energy of interaction is raised. This is especially true when the particle energies involved reach the relativistic region. However, particle selection in high-energy experiments also becomes more important as the interaction energy is raised, since more particles are produced and more types of particles are likely to be involved. In the case of an experiment where a "rare" particle is the object of the investigation, for example, one such particle is produced among a million others; the detector to be used here must possess a selectivity (generally called a rejection ratio) of at least  $10^{-7}$ —that is, the ability to reject  $10^7$  undesired particles for each desired one.

The detectors commonly used in high-energy investigations are cloud and bubble chambers, scintillation counters, Cerenkov counters, spark chambers, wire chambers, solid-state detectors, photographic emulsions, and others. These are all capable of detecting relativistic particles, but only a few are able to identify and select particles, especially in the relativistic energy region. A brief review is given here of those detectors which are capable of identifying (within certain limitations) and detecting particles in this region.

## Cloud and Bubble Chambers

Cloud and bubble chambers are among the most widely used tools in elementary particle research. Since charged particles produce visible tracks when they traverse the medium of the chamber (gases are used in cloud chambers, and liquids in bubble chambers), they provide an extremely useful means for observing the products of high-energy interaction processes. Usually the chamber is inserted inside a uniform magnetic field. By knowing the strength of the magnetic field, measuring the curvature of the particle track, and then counting the number of droplets in the ionized track, one can usually identify the particle which traverses the chamber.

An outstanding feature of these chambers is their good space resolution. With existing chambers, one can count on obtaining tracks 1 meter long or more. Sagittas of curved tracks can be measured in the chamber space with accuracies approaching 25 microns. The magnetic fields commonly used are of the order of 20 kilogauss, an intensity sufficient for measuring the momentum along a 100-Gev track with accuracy of 3 percent, but unsatisfactory for measurements at higher energies. The recent success in obtaining magnetic fields of 140 kilogauss with superconducting coils may make it possible to measure a 500-Gev track with accuracy about equal to the limit given by multiple coulomb scattering, although the angular measurements will not be correspondingly good. A liquid-hydrogen bubble chamber 14 feet (4.2 meters) in diameter, with a superconducting magnet, is being designed at Brookhaven for use with the alternating gradient synchrotron. With this bubble chamber the accuracy of momentum measurements will be considerably increased, because of greater length of the tracks, and very much increased for the particles that stop in the chamber. An artist's sketch of

this chamber is shown in Fig 1, with a sketch of the present 80-inch (200-centimeter) bubble chamber at Brookhaven, drawn to the same scale. The value of a large chamber, such as the proposed 14-foot chamber, lies not only in its increased accuracy but also in the completeness of the information it affords about the events observed. A chamber of this size would be very useful with a super-high-energy accelerator, such as the proposed 200-Gev or the 600- to 1000-Gev accelerator, especially if it were provided with a very strong magnetic field (for example, of the order of 100 kilogauss).

In bubble chambers, particle identification is usually accomplished by gap counting (that is, counting the number of gaps between adjacent droplets caused by ionization along the track); in cloud chambers it is accomplished by drop counting (counting the number of individual droplets). At very high energies in the relativistic region, determinations of  $\gamma$  ( $\approx 100$ ) to an accuracy of about  $\pm 10$  percent for tracks about 1 meter long are possible in heavy liquids, but in liquid hydrogen the achievable accuracy is only about  $\pm 30$  percent. Here

$$\gamma = (\sqrt{1 - v^2/c^2})^{-1}$$

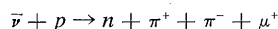
where  $v$  is the velocity of the particle and  $c$  is the velocity of light. In cloud chambers, notably when they are filled with xenon, an increase in ionization of 40 percent over the minimum rate has been observed at  $\gamma = 100$ , and of 70 percent at  $\gamma = 300$ . Such an increase in ionization with increasing energy of the particle after a minimum value at relativistic energy (called *minimum ionization*) has been reached is known as the "relativistic rise" effect. A typical ionization curve is shown in Fig. 2. By making use of the relativistic rise effect in addition to the other measurements mentioned above, it would be possible to identify particles at very high energies when the value of  $\gamma$  was in the neighborhood of several hundred, and perhaps even higher.

Complete analysis of events of the type that can be carried out at lower energies will be very difficult at relativistic energies, mostly because one must expect production of many neutral particles in addition to charged particles. Even in hydrogen, events will have to be treated statistically, rather than individually. Occasionally,

The author is on the staff of Brookhaven National Laboratory, Upton, New York.

individual particles will be recognizable. High-energy neutral particles decaying into charged particles with very short decay times would be observable. For a decay path of 2 millimeters, a particle of hyperon mass with 1000-Gev energy has lived about  $10^{-14}$  second. Thus, while complete analysis of production events will not be possible, production characteristics and properties of individual particles may still be determined in a number of instances.

The identification of specific relativistic particles in a bubble chamber can often be accomplished through modification of the chamber to accommodate various types of liquid or to incorporate metal plates inside the chamber. An example of this is the identification of the products of weak interaction events, either decays or neutrino interactions. Take a reaction such as



where  $\bar{\nu}$  is the antineutrino,  $\mu^+$  is the positive muon, and so forth; it is essential to know which particle is the muon. It is also important to be able to tell whether electrons are produced by some types of neutrino interactions. All these identifications can be accomplished by three particle-identification capabilities of a sufficiently large

bubble chamber (say, the 14-foot chamber being designed at Brookhaven); these capabilities are, (i) the trapping of charged particles; (ii) the identification of electrons by means of heavy metal plates; and (iii) the observation of neutral decays over a wide momentum interval.

Figures 3 and 4 are typical bubble-chamber photographs of interesting events which are identifiable. Figure 3 shows interactions of 5 Gev/c  $K$ -mesons. Figure 4 shows the production of a negative cascade hyperon, the  $\Xi^-$ , by an antiproton having momentum of 3.7 Gev/c.

### Spark Chambers

A spark chamber (1-3) generally consists of thin parallel conducting plates separated by small, and sometimes by large, gaps. The chamber is usually filled with neon or argon gas; a high-voltage electric pulse is applied to the plates, causing an electric discharge, or spark, to occur when a high-energy charged particle traverses the chamber.

A chamber operated with only two electrodes separated by a large gap—say, of the order of 50 centimeters—is generally known as a track spark chamber. If a track spark chamber is

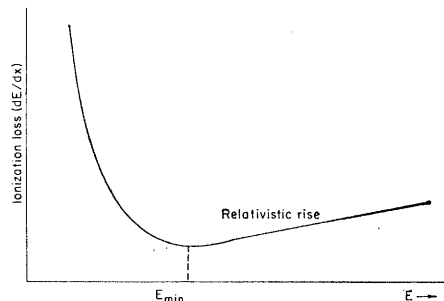


Fig. 2. Ionization curve.

operated with an electric field pulse of sufficiently high voltage to initiate short streamers along the path of a charged particle traversing the chamber, and if the pulse is of short enough duration to prevent the streamers from growing into a full-grown spark, the chamber is called a streamer chamber.

A track spark chamber is usually used within a magnetic field; it is similar to a bubble chamber and has certain advantages and disadvantages. One distinct advantage of a track spark chamber is that it has a very fast time resolution, as compared with a bubble chamber, and is easily triggered; thus it can be used conveniently in experiments requiring scintillation and Cerenkov counter systems for particle selection and other purposes.

At present, streamer chambers seem to hold greater promise for detection and identification of relativistic particles than other kinds of spark chambers. First, a streamer chamber has nearly isotropic sensitivity; second, ionization measurements can be made with more precision in a streamer chamber than in other types of chambers; and third, a large number of simultaneous tracks can be detected. However, measurements of absolute ionization in streamer chambers lack the precision obtainable in a bubble chamber. The ultimate limit in the momentum determination of a traversing particle in 1-meter streamer tracks in a magnetic field of 10 kilogauss is estimated to be 400 Gev/c (2, 4).

### Cerenkov Counters

During the past two decades the most widely used and most accurate method for detecting and identifying charged particles in the relativistic region has been the appropriate utilization of the Cerenkov radiation.

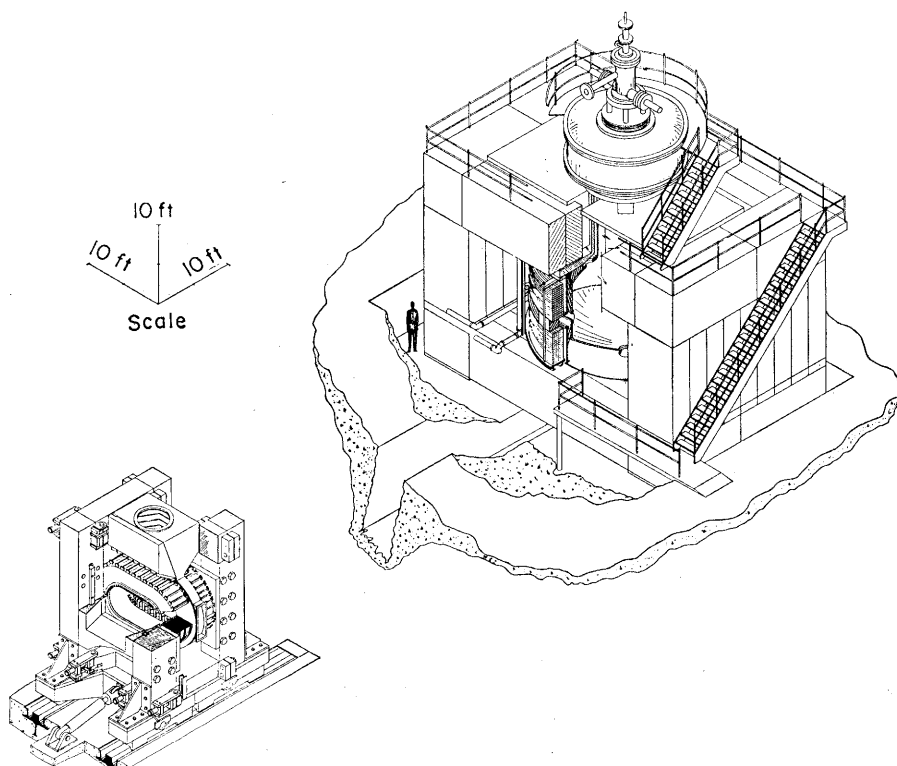


Fig. 1. Artist's sketch of the contemplated 14-foot bubble chamber, with the present 80-inch bubble chamber at Brookhaven shown for comparison.

A Cerenkov counter (5-7) can be constructed from any relatively transparent optical medium which possesses an index of refraction greater than 1 in the region of the visible spectrum. Cerenkov radiation is emitted when a charged particle traverses the medium with a velocity,  $v$ , greater than the velocity of light,  $c$ , in the medium. The emitted photons are radiated along the elements of conical surfaces of angle  $\theta$  relative to the direction of motion of the particle, where  $\theta$  is given by

$$\cos \theta = \frac{1}{\beta n(\nu)} \quad (1)$$

Here,  $\beta$  is the ratio of the particle velocity to the velocity of light in a vacuum, and  $n(\nu)$  is the optical index of refraction of the medium at the frequency  $\nu$  of the emitted photon.

From Eq. 1 one can see that the detection of Cerenkov light sets a threshold for  $\beta$ ; that is,  $\beta > 1/n$ . There-

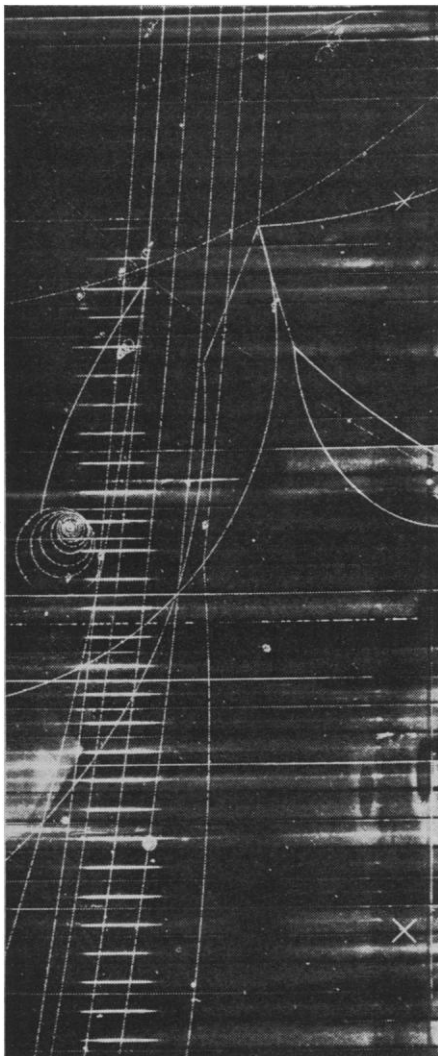


Fig. 3. Photograph of interactions of  $K^-$  mesons of momentum 5 GeV/c.

fore, particles with velocity  $\beta < 1/n$  will not emit Cerenkov light, and a detector can easily be made with a radiator medium chosen for its appropriate refractive index,  $n$ , so that only particles above the threshold velocity are detected. Such a Cerenkov detector is called the threshold detector. For example, a threshold detector with a gas medium having, at normal pressure, a refractive index close to 1 is commonly used to detect only particles of  $\beta \approx 1$ —that is, particles in the relativistic region. The threshold of this type of detector is generally not sharp enough to provide sufficient resolution for the separation of particles with velocities close to each other. A focusing type of Cerenkov counter, also known as a differential Cerenkov counter, is most widely used; it has an exceedingly high resolution and is used to identify and separate particles with velocities very close to each other, such as are generally encountered in the relativistic region. Figure 5 is a schematic drawing of a typical focusing counter using a liquid-containing cell as radiator.

A further example is that of a very useful counter employing carbon dioxide gas as the radiator. Its optical system is so adjusted that Cerenkov radiations emitted at  $\theta = 5^\circ$  are accepted. It consists of a spherical concave mirror having a focal length of 42 inches; a plane mirror, placed at  $45^\circ$ , for bringing the light out of the particle beam; and a specially shaped conical mirror for concentrating the light transmitted by the annular slit onto the photocathode of a photomultiplier tube. The angular resolution, as defined by the annular slit, is 0.009 radian. The velocity resolution of this counter is  $\Delta\beta \approx 8 \times 10^{-4}$ . In order to improve the rejection ratio—the ratio of desired to undesired particles—the Cerenkov light emitted by the undesired particles as well as by the desired particles is collected simultaneously in the same counter. This light is collected in separate channels, and the Cerenkov light from the desired particles is used in coincidence with signals usually derived from the other elements of a counter telescope, whereas the light from the undesired particles is used in anticoincidence with these signals. A typical analysis of a negative beam of momentum 8.5 GeV/c at a laboratory production angle of  $\sim 4\ 3/4^\circ$ , from the Brookhaven alternating-gradient synchrotron, is shown in Fig. 6.

Since the limiting factor in the practical design of a focusing-type Cerenkov counter is the minimum intensity of the Cerenkov light detectable over the noise background of the photomultiplier tube used, it is imperative to require a certain minimum detectable light output when varying the design parameters of the counter to achieve the maximum obtainable resolution. In a focusing type of Cerenkov counter, the velocity resolution is expressed by the equation

$$\frac{\partial \theta}{\partial \beta} = \frac{1}{\beta^2 n \sin \theta} \quad (2)$$

The velocity resolution is inversely proportional to  $\sin \theta$ , whereas the intensity of Cerenkov radiation per unit frequency interval and per unit path length is proportional to  $\sin^2 \theta$  and is given by

$$\frac{d^2 N}{dx dv} = \frac{2\pi Z^2}{137c} \sin^2 \theta \quad (3)$$

where  $\nu$  is the frequency of emitted photons and  $Z$  is the ratio of the magnitude of the charge of the moving particle to the magnitude of the electronic charge. In order to improve the resolution of a focusing counter, one must decrease the angle  $\theta$ , but then the intensity of the Cerenkov radiation decreases much more rapidly with  $\theta$ —that is, it decreases with  $\sin^2 \theta$ .

Thus the usefulness of Cerenkov counters for identification and separation of particles, because of intensity consideration alone, is limited to experimental applications in

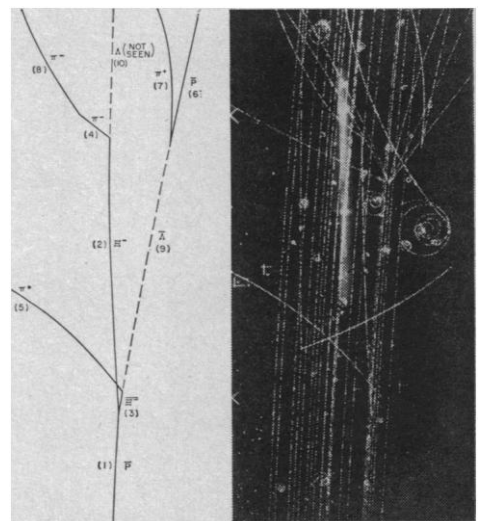


Fig. 4. Production of a negative cascade hyperon,  $\Xi^-$ , by an antiproton of 3.7 GeV/c.

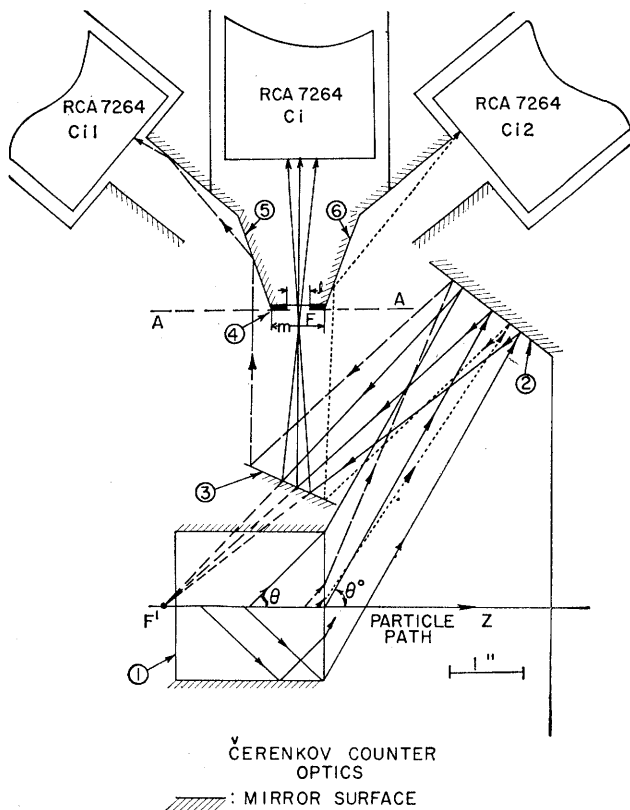


Fig. 5. Schematic drawing of a Cerenkov counter.

the energy region probably not exceeding momentum of 200 Gev/c. There are other factors which may affect the ultimate resolution obtainable in these counters, such as the dispersion effect in the medium and scattering of the particles (multiple Coulomb scattering and diffraction scattering). Corrections of the dispersion effects in a gas differential counter have been obtained (6-8) by means of special lenses, and resolution has thus been increased by a factor of  $\sim 20$ . At very high energies the scattering effect is very small, and in most applications it is not a serious effect and can be ignored.

### Cerenkov Chambers

As expressed in the simple relation of Eq. 1, the Cerenkov light is emitted at an angle  $\theta$  to the trajectory of a charged particle; the light in any one plane can be focused in the focal plane of a lens (see Fig. 7). The resultant image of the Cerenkov light appears as a circle because of optical symmetry about the optical axis. The radius of such an image circle is related to  $\theta$  and the focal length of the lens,  $f$ :

$$r = f \tan \theta \quad (4)$$

In a beam of particles, if all particles are parallel and traversing the medium in the same direction along the optical axis and with the same velocity, then one will get a single ring image with a radius  $r$ . However, if a particle traverses the medium in a direction not parallel to the optical axis, but inclined to it at an angle  $\delta$ , the radius of the image ring is, to a first order, unchanged, but the center of the ring is moved off-axis by an amount

$$d = f \tan \delta$$

If a light-sensitive mosaic screen is placed in the focal plane of the lens and is capable of detecting the position of the ring as well as the magnitude of its radius, it is possible to determine not only the velocity of the particle but the direction of its trajectory also. However, since the intensity of the Cerenkov radiation is usu-

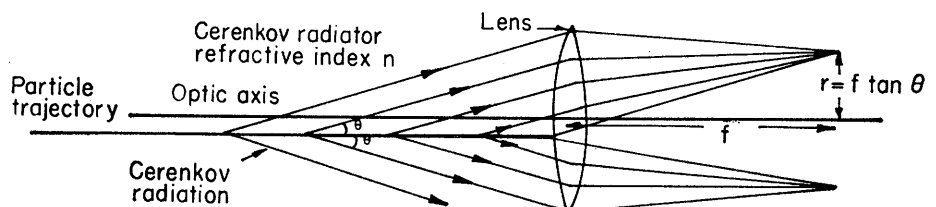


Fig. 7. Cerenkov light rays.

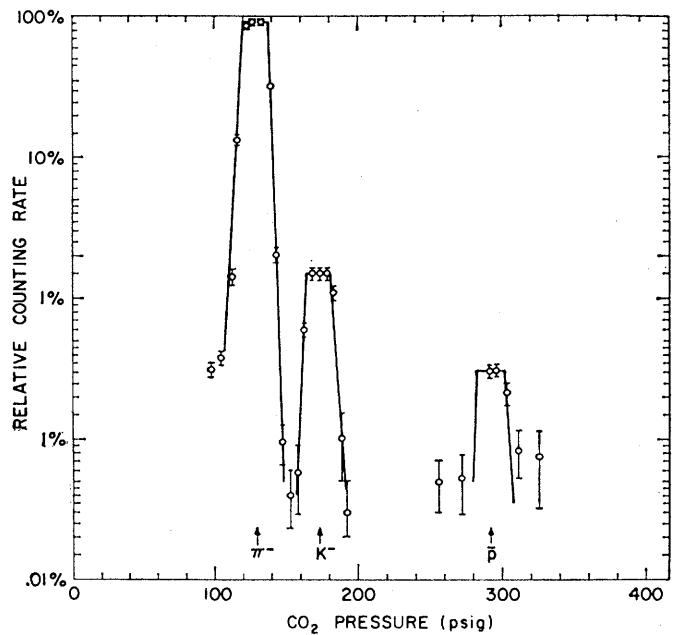


Fig. 6. Spectrum of particles obtained in a gas differential Cerenkov counter.

ally low, each element of light received on the screen is extremely weak and must be amplified enough so that accurate measurements of the velocity and direction of the traversing particle can be made. A detector of this kind was constructed recently, and measurements have been made of the velocities of protons of 5.8-GeV energy through detection of the ring images produced (9). A high-gain image-intensifier tube was used in the detection of the image ring.

Figure 8 is a schematic diagram of such a Cerenkov chamber. The chamber consists of a gas-containing pressure vessel with a long flight tube along which the charged particle traverses the medium and emits Cerenkov radiation. The radiator used is a high-pressure gas having an index of refraction of  $\sim 1.01$  to  $1.03$ . The light is deflected by a  $45^\circ$  mirror and then passes through a window and through

a lens which focuses it into a ring image on the photocathode of the image intensifier. Figure 9 shows a ring image obtained in such a chamber with an accumulated signal from 500 protons of 5.8-Gev energy. Figure 10 shows the image from a single proton.

The velocity precision obtainable at all the ring radii considered is expressed as a standard deviation,

$$\frac{\delta\beta}{\beta} \approx \pm 2 \times 10^{-4}$$

The precision with which the position of a ring, in terms of its central coordinates, can be measured varies from 3 to 9 milliradians, according to the different numbers of spots available to define the ring.

### Relativistic-Rise Detectors

The ionization produced by a charged particle traversing low-density media such as gases rises logarithmically with increasing energy above the minimum ionization energy. This is the well-known relativistic rise (6, 7), and it can be seen in the equation

$$-\frac{dE}{dx} = \frac{2\pi n z^2 e^2}{m v^2} \times \left[ \ln \left( \frac{2 m v^2 W_{\max}}{I^2 (1 - \beta^2)} \right) - 2\beta^2 - \delta - U \right] \quad (5)$$

where  $dE/dx$  is the ionization loss of a particle of charge  $z$  in traversing a substance;  $n$  is the number of electrons per cubic centimeter in this substance;  $m$  is the electron mass;  $v$  is the velocity of the particle;  $\beta = v/c$ ;  $I$  is the mean excitation potential of the atoms of the substance;  $W_{\max}$  is the maximum energy transfer from the incident particle to the atomic electrons;  $\delta$  is the correction for the density effect due to the polarization of the medium; and  $U$  is a term due to the nonparticipation of the inner shells ( $K, L, \dots$ ) for very low velocities of the incident particle.

In the relativistic region, the denominator  $(1 - \beta^2)$  in the logarithm term of Eq. 5 results in a logarithmic increase of  $dE/dx$  with increasing energy. The relativistic rise is reduced in denser materials, such as solids, because of the screening of the Coulomb field by the close packing of the atoms. This is known as the density effect.

Since the identification of particles having energies extending well into

the relativistic region becomes more difficult with increasing energy, it is worthwhile to look into the possibility of making use of such a relativistic rise effect for identification of the desired particles in this energy region.

From Eq. 5 one can easily see that, if the density effect is not present, the separation of the ionization peaks due to the presence of two relativistic particles of different mass but the same momentum is independent of the momentum region of the particles. It is expected that this will apply to high-energy particles in the many-hundred-Gev region.

There are several possible approaches which look promising—for example, xenon scintillation counters, transition radiation detectors, and secondary-emission detectors.

**Xenon scintillation counters.** Since xenon was found to be the best available scintillating gas, a xenon gas-scintillation counter (6, 7) 1 meter long and with a pressure of 1.5 atmospheres has been tested in a momentum-analyzed secondary beam at the Brookhaven 33-Gev alternating-gradient synchrotron in coincidence with a counter telescope consisting of scintillation detectors and a focusing-type Cerenkov counter. The pressure of the xenon is low enough so that the "density" effect is negligible within the momentum range tested. Results obtained on the pulse-height distribution of the signal output from the xenon counter as selected by the Cerenkov counter (either pions or protons) show the characteristic Landau distribution. The peak of the spectrum for negatively charged pions with momentum of 12 Gev/c, shows a large increase in the ionization loss compared with that for negative pions with momentum of 7 Gev/c, and a clear separation of the two peaks is obtainable. Similar results, with a clear separation of the spectrum peaks, were also obtained for positively charged pions with momentum of 4 Gev/c ( $\gamma \approx 30$ ) and protons with momentum of 7 Gev/c ( $\gamma \approx 7$ ).

With an array of such gas counters—say, a ten-section scintillation train 30 meters in overall length filled with xenon at pressure of 1 atmosphere—pion-proton separation can be expected at momentum of 100 Gev/c and perhaps at 200 Gev/c.

**Transition radiation detectors (1, 10).** The existence of transition radia-

tion—that is, electromagnetic radiation emitted by a charged particle traversing the boundary between two media—was predicted as early as 1945 (11). The electromagnetic field of a moving charge has an image field due to the presence of the boundary. When the charged particle moves toward the boundary, its electromagnetic field moves closer to its image field. At the instant the charged particle crosses the boundary there is a

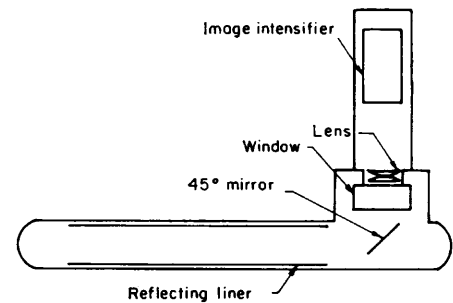


Fig. 8. Schematic drawing of a Cerenkov chamber.

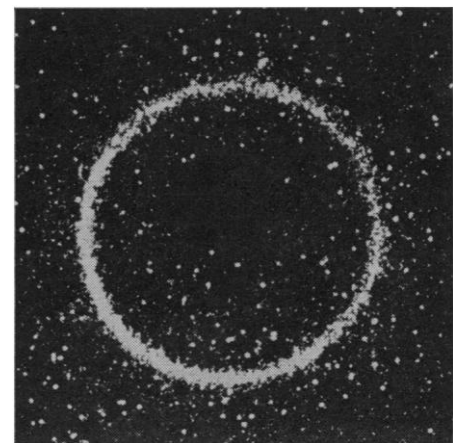


Fig. 9. Photograph of a Cerenkov ring for 500 protons.

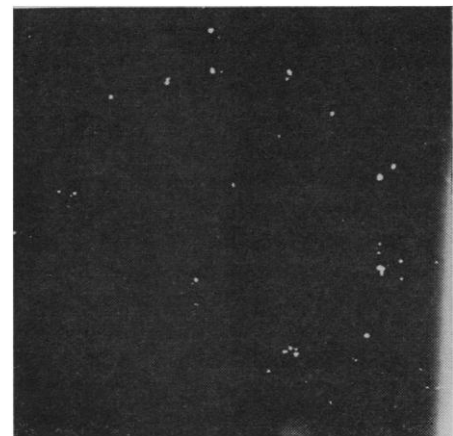


Fig. 10. Photograph of a Cerenkov ring for 1 proton.

sudden collapse of the two fields, and this gives rise to a loss of energy. This loss of energy is in the form of electromagnetic radiation, which is known as transition radiation.

The intensity per unit solid angle,  $dI/d\Omega$ , of the transition radiation for a particle of charge  $e$  and velocity  $c$ , incident normally on the boundary between vacuum and a medium of complex dielectric constant  $\epsilon$ , is given by Eq. 6 (see below), where  $\theta$  is the angle of the radiation with respect to the normal to the boundary. The radiation is plane-polarized in the plane defined by the incident charged particle and the out-going photon.

For nonrelativistic particles the intensity of the transition radiation is proportional to the kinetic energy of the particle. However, for relativistic particles the intensity is no longer a linear function of the particle energy, but is much more complicated. With certain approximations, Garibian (12) has evaluated Eq. 6 for the x-ray spectrum of the transition radiation. The main conclusions for the x-ray spectrum are as follows.

1) The radiation is zero in the direction of the particle trajectory but increases extremely rapidly with a slight increase in angle and reaches a sharp peak in the radiation pattern.

2) The yield in the number of photons is proportional to the square of the particle energy ( $\gamma = E/mc^2$ ).

3) The transition radiation is not affected by the density effect.

For the optical spectrum of the transition radiation at relativistic energies, the evaluation of Eq. 6 becomes much more involved, and no clear-cut conclusion is yet available (13).

Experimental observation of the transition radiation has been accomplished both for nonrelativistic particles (14) with a proton beam of energy between 1 and 4.5 Mev, and for relativistic particles with relativistic electrons from a beta source as well as from high-energy muons in cosmic rays (1).

The energy dependence characteristic of the transition radiation in the relativistic region (at least for the x-ray spectrum) suggests the possibility of using this radiation for measuring energies of relativistic particles. Un-

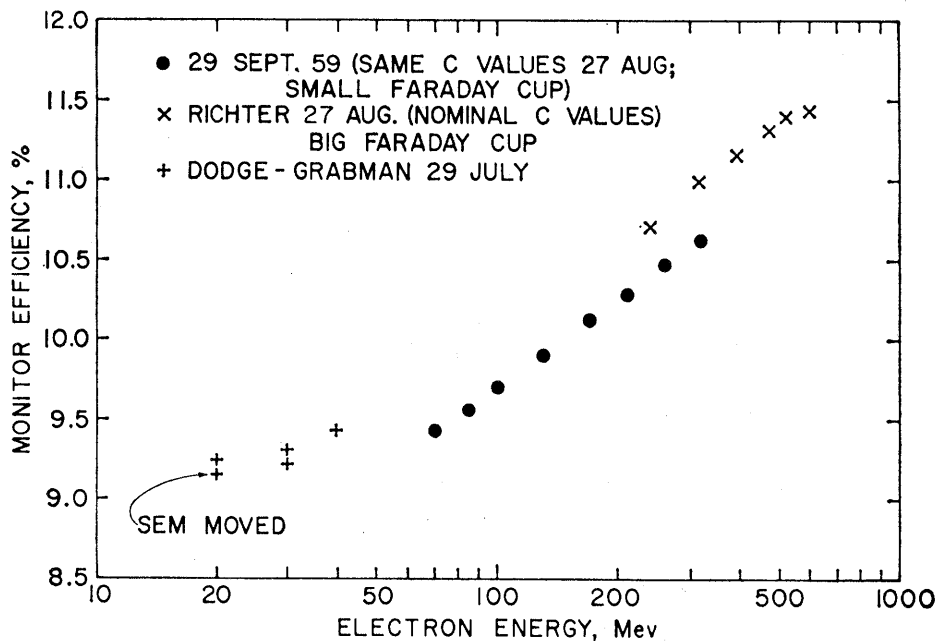


Fig. 11. Relativistic rise effect in a secondary emitter.

fortunately, the intensity of the transition radiation is extremely low, and for single-particle detection a large number of transition layers is necessary to produce enough photons for possible detection. Extensive studies are being made with both the optical spectrum and the x-ray spectrum in an effort to develop transmission-radiation detectors of simple charged particles.

*Secondary-emission detectors.* When a charged particle passes through a thin conductor, its electromagnetic field interacts with the atoms at the surface, causing secondary-emission electrons to be ejected from the surface. If the particle velocity reaches the relativistic region, then the electromagnetic field contracts in the direction of motion of the particle but the field extends farther from the direction of motion, hence causes more secondary emission from elements of the surface farther away. This phenomenon is very similar to the relativistic rise in the ionization loss of a charged particle traversing a medium, except that it is entirely a surface effect and may be of a more complicated nature.

Evidence showed (15) that a secondary emission exhibits a relativistic rise when electrons impinge on thin metal foils. These results showed that the secondary-emission current caused

by an electron beam increases logarithmically with the electron energy between 40 Mev ( $\nu = 80$ ) and 600 Mev ( $\nu = 1200$ ) (see Fig. 11). No density effect was evident, possibly because a surface phenomenon is involved. Similar relativistic rise effects have also been observed in very thin scintillators (1).

The main difficulty with this kind of detector was the extremely low efficiency for secondary emission at high energies of the material investigated prior to 1965. It was estimated that, in order to separate, at  $\nu = 50$ , a single pion from a muon, about 2000 to 3000 secondary-emission foils would be needed for the best secondary-emitter material available at that time. Recently, Edgecumbe and Garwin (16) have found new materials, appropriately processed, which are extremely good secondary emitters at high energies ( $\sim 500$  Mev), with a remarkably high efficiency, hundreds of times higher than that obtainable with conventional material. The new materials tested include highly porous but very thin films of potassium chloride, cesium iodide, and other compounds. Experimental tests in an electron beam in the 500-Mev energy range showed a relativistic rise effect similar to the results obtained by Richter *et al.*, as shown in Fig. 11. With the tremendous increase in secondary-emission efficiency obtainable with the new materials, it is hoped that secondary-emission detectors can

$$\frac{dI}{d\Omega} = \frac{e^2\beta^2}{\pi^2c} \frac{\sin^2\theta \cos^2\theta}{(1 - \beta^2 \cos^2\theta)^2} \int_0^\infty \left| \frac{(\epsilon - 1) [1 - \beta^2 + \beta(\epsilon - \sin^2\theta)^{\frac{1}{2}}]}{[(\epsilon \cos\theta + (\epsilon - \sin^2\theta)^{\frac{1}{2}}) [1 + \beta(\epsilon - \sin^2\theta)^{\frac{1}{2}}]]} \right| d\omega \quad (6)$$

be constructed to detect and identify individual charged particles at ultrarelativistic energies.

A specially designed photomultiplier tube incorporating the new material as the secondary-emission cathode is being constructed for detailed studies of possible single particle detection.

## Conclusions

It appears possible to extend the application of most of the existing detection techniques to the identification and separation of charged particles in the relativistic energy region. One can probably extend these applications, in certain limited cases, up to an energy region of several hundred billion electron volts. However, for general applications in the identi-

fication of particles in the ultrarelativistic region, the existing detectors are rather limited, and new methods and approaches are desirable. At present, detectors making use of the relativistic rise effect seem to show considerable promise.

## References and Notes

1. A. I. Alikhanian, Loeb Lecture notes, Harvard University, Feb. 1965.
2. K. Strauch, *IEEE (Inst. Elec. Electron. Engrs.) Trans. Nucl. Sci.* **12**, No. 4, 1 (1965).
3. W. A. Wenzel, *ibid.* **13**, No. 3, 34 (1966).
4. G. E. Chikovani, V. N. Roinishvili, V. A. Mikhailov, *Nucl. Instr. Methods* **29**, 261 (1964); *Soviet Phys. JETP (English Transl.)* **19**, 833 (1964); F. Bulos, A. Boyarski, R. Diebold, A. Odian, B. Richter, F. Villa, *IEEE (Inst. Elec. Electron. Engrs.) Trans. Nucl. Sci.* **12**, No. 22 (1965).
5. L. C. L. Yuan and C. S. Wu, in vol. 5A of *Nuclear Physics* (Academic Press, New York, 1962).
6. J. P. Blewett and L. C. L. Yuan, Eds., "Experimental Program Requirements and Design Study for a 300-1000 BeV Accelerator," *Brookhaven Nat. Lab. Rep. BNL 772* (1962).
7. L. C. L. Yuan, Ed., "Nature of Matter—Purposes of High Energy Physics," *Brookhaven Nat. Lab. Rep. BNL 888* (1965).
8. R. Meunier, J. P. Stroot, B. Leontic, A. Lundby, *Nucl. Instr. Methods* **17**, 1 (1962).
9. P. Iredale, G. W. Hinder, D. J. Ryden, A. G. Parham, *IEEE (Inst. Elec. Electron. Engrs.) Trans. Nucl. Sci.* **13**, 399 (1966).
10. F. W. Inman and J. J. Muray, *ibid.*, p. 373.
11. I. M. Frank and V. L. Ginsburg, *Soviet Phys. JETP (English Transl.)* **16**, 15 (1945).
12. G. M. Garibian, *ibid.* **33**, 1403 (1957); *ibid.* **6**, 1079 (1958); *ibid.* **8**, 1003 (1959); *ibid.* **10**, 372 (1960).
13. A private communication from A. I. Alikhanian of the Physical Institute of the Armenian Academy of Sciences informed the author that A. Amatuni and G. Garibian of his institute had worked out some of the behaviors of the transition radiation in the optical region. They found that in a certain limited frequency region the intensity of transition radiation is a function of the 4th power of the particle energy, whereas in other frequency regions it exhibits a logarithmic dependence on the energy.
14. P. Goldsmith and J. V. Jelley, *Phil. Mag.* **4**, 836 (1959).
15. B. Richter, H. C. deStaebler, W. R. Dodge, Grabman, data presented in 6.
16. J. Edgecombe and E. L. Garwin, "U.S. Atom. Energy Comm. Publ. SLAC-PUB-166," in press.
17. Work performed under the auspices of the U.S. Atomic Energy Commission.

## NEWS AND COMMENT

# The Smale Case: NSF and Berkeley Pass Through a Case of Jitters

To savor the pungency of the events about to be related, it is necessary to be mindful of the bruised condition of the two institutions that are central to the story. First there is the National Science Foundation, which has an instinct for trouble-avoidance derived from 15 years of congressional badgering, budget slashing, and allegations that NSF's clients have been living it up or pursuing esoteric nonsense at the taxpayers' expense. Then there is the academic world's leading convalescent, the Berkeley campus of the University of California, where the fragile peace that ended nearly 2 years of debilitating strife is now being sniped at from the right by Ronald Reagan, the Republican candidate for governor. If administrators at NSF and Berkeley are edgy and cautious, who can blame them?

With this backdrop in place, it is time to introduce the central figure of the story, Stephen Smale, age 36, of the mathematical species known as differential topologist, and of the political species known as left-wing activist. Seven years ago Smale achieved an

enduring place in topology by developing a theory for turning a sphere inside out without creasing it, let alone cutting it. But the matters that we are concerned with here relate to Smale's recent role in turning Berkeley and NSF inside out, the former being the place where he holds a tenured professorship in mathematics, and the latter being the source of a \$91,500 grant, which, as principal investigator, he shares with some 15 other mathematicians. Let us go back a bit and trace the complex train of events in the Smale affair.

Despite his courteous mien, soft speech, and scholarly dedication, Stephen Smale long ago became practiced in speaking out or acting on his convictions when he doesn't like what's going on around him. In high school he agitated against a ban on teaching evolution. As an undergraduate at the University of Michigan, he was put on probation for refusing to cooperate in an investigation of a private dinner that was held for a speaker who had been barred from the campus. But along the way he was also, as the expression

goes, "doing mathematics" and mathematics of a most distinguished sort. In 1961, an appointment to Columbia is said to have made him the youngest full professor on any major campus in the country.

In 1964, Berkeley, the mecca of mathematics and academic political activism, beckoned, and Smale went west. He naturally was involved in the Free Speech Movement, and later went on to co-found the Vietnam Day Committee, whose climactic act, last October, was intended to be a demonstration aimed at stopping troop trains. But, as Smale said in an interview with *Science*, he was deeply disappointed when the marchers did not attempt to cross the police cordons. "After all the buildup, the tactic of turning away left people feeling demoralized," he explained. Motivated in part by disappointment over what he considered to be a lack of militancy among his Vietnam Day Committee associates, Smale pretty much dropped out of the movement, and nothing was thereafter publicly heard of him until this past summer. Then began a complex series of events that was to make Smale probably the best known topologist of all time.

At the end of the last academic year, Smale, as is not uncommon in the academic community, embarked on an extensive work and vacation trip, the culmination of which, in his case, was to be the International Congress of Mathematicians, in Moscow, starting 16 August. There he was to deliver a paper and receive the Fields award,